LIMNOLOGY and OCEANOGRAPHY LETTERS



Open Access

Limnology and Oceanography Letters 2025

© 2025 The Author(s). Limnology and Oceanography Letters published by Wiley Periodicals LLC
on behalf of Association for the Sciences of Limnology and Oceanography.
doi: 10.1002/lo12.70055

LETTER

Emergent seasonal hypoxia and acidification risks induced by seaweed and fish polyculture in the world's largest seaweed farm

Yanmei Liu, ^{1,2†} Wei Yang ^{1,2†} Yingxu Wu ^{1,2,3*} Wei-Jun Cai ^{1,2} Chenglong Li, ^{1,2} Hongyang Lin, ⁵ Peiqiang Zhuang, ^{1,2} Jianhang Zhang, ^{1,2} Yifan Xu, ^{1,2} Huaji Qiu, ³ Youjun Huang, ⁶ Di Qi^{1,2*}

¹State Key Laboratory of Mariculture Breeding, Jimei University, Xiamen, China; ²Polar and Marine Research Institute, College of Harbour and Coastal Engineering, Jimei University, Xiamen, China; ³Xiamen Lantan Space Technology Company, Xiamen, China; ⁴School of Marine Science and Policy, University of Delaware, Newark, Delaware, USA; ⁵State Key Laboratory of Marine Environmental Science, College of Ocean and Earth Sciences, Xiamen University, Xiamen, China; ⁶Xiamen Identity Treasure Network Technology Company, Xiamen, China

Scientific Significance Statement

Seaweed farming is increasingly recognized as a promising strategy for marine carbon dioxide removal (mCDR). However, its ecological sustainability, particularly in semi-enclosed bays, remains uncertain. Using data collected from Sansha Bay, Fujian, China, the world's largest seaweed farming site, our study reveals an inherent trade-off: in highly sheltered coastal environments, especially when integrated with algae-fish polyculture, seaweed farming can induce significant hypoxia and acidification risks through organic carbon degradation. Carbon isotopic tracing further demonstrates that seasonal shifts in organic carbon sources—from fish feed in autumn to macroalgal detritus in spring—diminish the potential of macroalgal-based carbon sequestration. These findings emphasize the complexity of coastal carbon management and highlight the critical importance of considering ecosystem health—including the system's capacity to maintain oxygen and pH stability and sustain biogeochemical functioning—when implementing seaweed-based carbon sequestration strategies.

Abstract

Seaweed farming is increasingly promoted as a carbon sequestration strategy, but its effectiveness relies on carbon burial and export to deep waters. Seaweed farms commonly occupy semi-enclosed bays, causing continuous accumulation of organic carbon (OC) and its degradation products, potentially undermining carbon sequestration and driving hypoxia and acidification. These ecological impacts may be amplified in fish-algae polyculture systems, yet they remain unclear. We investigated carbon cycling in Sansha Bay, China, the world's largest seaweed farm and intensive algae–fish polyculture site. During aquaculture seasons, bottom waters experienced rapid OC decomposition, causing severe oxygen depletion and acidification. Vertical mixing spread these effects throughout the water column, turning surface waters into net $\rm CO_2$ sources. $\delta^{13}C_{\rm DIC}$ carbon isotopic analyses indicated seasonal shifts in dominant OC sources, from fish feed in autumn to macroalgal detritus

This is an open access article under the terms of the Creative Commons Attribution License, which permits use, distribution and reproduction in any medium, provided the original work is properly cited.

[†]These authors contribute equally

Associate editor: Dongyan Liu

^{*}Correspondence: yingxu.wu@jmu.edu.cn; qidi@jmu.edu.cn



in spring. These findings underscore the importance of evaluating the sustainability of coastal systems when pursuing seaweed-based carbon sequestration.

The ocean absorbs approximately 26% of anthropogenic CO_2 emissions, playing a crucial role in climate regulation (Friedlingstein et al. 2025; Gattuso et al. 2015). Marine carbon dioxide removal (mCDR) strategies aim to enhance the ocean's capacity to sequester additional CO_2 , representing promising approaches to mitigate global warming (Doney et al. 2025). Among these, large-scale seaweed farming (e.g., macroalgae cultivation) has attracted considerable attention due to its rapid biomass production and subsequent organic carbon export and potential carbon sequestration (Duarte et al. 2021, 2025; Krause-Jensen and Duarte 2016; Krause-Jensen et al. 2018; Paine et al. 2021).

Macroalgae function as crucial carbon sinks, but their effectiveness depends on the efficient transport of organic carbon and its long-term storage and net inventory increase in deep ocean reservoirs (Krause-Jensen and Duarte 2016; Filbee-Dexter et al. 2024). In open coastal systems with wild algal forests, persistent tidal forcing and turbulent mixing can export algal detritus offshore, where it settles into deep waters under gravitational forcings. This process not only prevents local organic matter accumulation but also enhances long-term carbon burial via effective cross-shelf particulate export. In contrast, seaweed farms are often established in semi-enclosed bays characterized by limited water exchange and thermally stable conditions. While these conditions favor robust macroalgal growth, they also lead to the prolonged retention of degraded biomass within the system (Han et al. 2024; Wang et al. 2023). The resulting elevated nutrient concentrations and accumulation of organic debris stimulate intense microbial activity, accelerating further decomposition processes that consume dissolved oxygen (DO) and release CO2. This cascade ultimately triggers hypoxia and acidification events with significant ecological consequences (Bach et al. 2021; Gallagher et al. 2022; Xiong et al. 2024).

Previous studies specifically addressing hypoxia and acidification risks associated with seaweed farming remain limited. Nonetheless, analogous phenomena in natural, algaedominated ecosystems offer valuable insights. For instance, in Chesapeake Bay—a system prone to seasonal hypoxia—oxygen depletion is primarily driven by phytoplankton blooms followed by subsurface and benthic decomposition (Du et al. 2018; Officer et al. 1984; Zheng and DiGiacomo 2020; Su et al. 2020). Similarly, bottom waters of larger riverimpacted coastal oceans such as those on the northern Gulf of Mexico (United States) and the East China Sea (China) receive substantial organic carbon input (70%–80%) from surface algal blooms, whose rapid decomposition dramatically reduces DO levels (by 90%–111%) and triggers mass mortality events (Jiang et al. 2014; Wang et al. 2017; Wang

et al. 2016, 2018; Zhang et al. 2022;). Given that transient algal proliferation in these natural systems can induce severe hypoxia and acidification, similar—or even amplified—risks are highly likely in semi-enclosed aquaculture environments characterized by limited water exchange and intensive polyculture practices.

Integrated multi-trophic aquaculture models conceive synergistic relationships where fish consume macroalgal detritus and macroalgae assimilate CO_2 released by fish respiration (McNeary and Erickson 2013; Saba et al. 2021). However, empirical evidence indicates that only about 20%–25% of fish feed is utilized by cultured organisms (Han et al. 2021; Hu et al. 2012), leaving behind substantial organic residues. These residues further elevate oxygen demand and disrupt the carbonate chemistry of the system. Despite these findings, critical knowledge gaps persist regarding the temporal dynamics and predominant sources of organic matter driving hypoxia and acidification in intensive polyculture aquaculture systems.

We conducted comprehensive biogeochemical investigations in Sansha Bay, China—a representative seaweed farming system that produces approximately 1.8 million tons of biomass annually (fresh weight; Duarte et al. 2025). Notably, Sansha Bay features a narrower opening and greater physical barriers compared to a typical semi-enclosed bay (Fig. 1a,b), making it a highly sheltered system that experiences significantly restricted water exchange with the open ocean (Han et al. 2021; Lin et al. 2017, 2019). Aquaculture activities in this region follow a well-defined seasonal pattern, with macroalgae (e.g., Saccharina japonica) cultivated mainly from winter through spring and intensive fish farming occurring in spring and autumn (see details in Methods), coinciding with periods of high feed input and organic matter loading (Deng et al. 2025; Xie et al. 2021). By integrating carbonate parameters measurements, $\delta^{13}C_{DIC}$ isotopic tracing, and end-member mixing analyses, we compared carbon biogeochemical cycling in seaweed culture, seaweed-fish polyculture, and non-culture. Our quantitative assessment of the contributions from macroalgal detritus and fish feed decomposition to subsurface CO2 release uncovers the mechanisms driving hypoxia and acidification in seaweed farms with highly restricted water exchange.

Materials and methods

Study area and aquaculture types

Sansha Bay (26°30′–26°58′N, 119°26′–120°10′ E), located in the northeastern Fujian Province, China, is a lagoon-like semi-enclosed coastal system spanning approximately 675 km². An area of 150 km² within the bay is designated for seaweed farming (Fig. 1c–g), making it the world's largest contiguous macroalgae cultivation zone (Duarte et al. 2025). The bay connects to the East China Sea via the narrow Dongchong

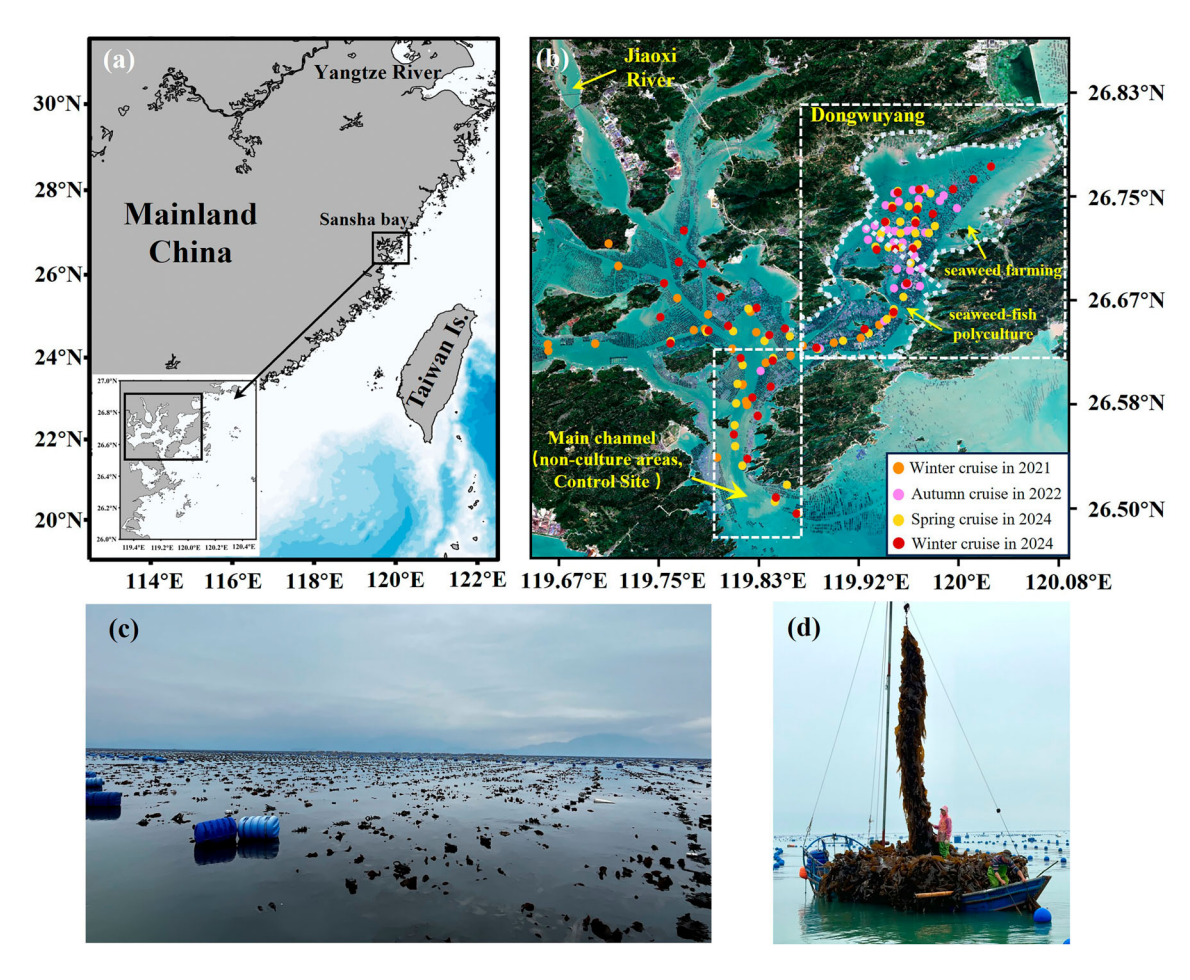


Fig. 1. Map of Sansha Bay and the seaweed farming activities within the bay. (a) Geographic location of Sansha Bay. (b) Sampling stations during four cruises. (c) Macroalgae cultivation areas. (d) Operational harvesting processes for seaweed.

Channel (3 km width; Figs. 1, 2i) (Ji et al. 2021; Lin et al. 2017; Xie et al. 2022). The bay's unique topography limits water exchange, predominantly driven by tidal action (Fig. 1a,b). Hydrodynamic studies show spatially variable exchange rates, with half-exchange times less than 10 d in the main channel but significantly longer (15–40 d) in the inner Dongwuyang region (Lin et al. 2017, 2019). As a consequence, this system exhibits high sedimentation rates but significantly lower stocks of organic carbon in sediments (Duarte et al. 2025).

Aquaculture activities in Sansha Bay exhibit clear spatial variability, primarily comprising raft-based and cage-based aquaculture systems (Fig. 1c–g). Macroalgae cultivation focuses predominantly on *S. japonica* (December–May) and *Gracilariopsis lemaneiformis*, the latter of which, despite its shorter culture cycle, is cultivated nearly year-round (Deng et al. 2025). Simultaneously, cage farming of *Larimichthys crocea* follows two intensive stocking cycles annually (April–May and October–December), demanding substantial feed inputs (Wang et al. 2024; Xie et al. 2021). During our surveys, *G. lemaneiformis* and *L. crocea* dominated in

autumn; *G. lemaneiformis* alone was cultivated in winter (as *S. japonica* had not yet been deployed), and *S. japonica* became dominant in spring when it entered the harvest stage (Supporting Information Fig. S1; Supporting Information Tables S1–S3). The integration of intensive polyculture practices with limited hydrodynamic exchange renders Sansha Bay an ideal natural laboratory for investigating carbonate chemistry alterations under sustained aquaculture and organic matter enrichment.

Sampling and data collection

Four seasonal surveys were conducted in winter 2021 (December 11–12), autumn 2022 (November 17–19), spring 2024 (April 4–7), and winter 2024 (December 1–4) (Fig. 1). Water samples were collected using 5 L Niskin bottles, immediately transferred to 250 mL PYREX borosilicate glass bottles, and poisoned with 100 μL of saturated HgCl $_2$ solution for subsequent analysis of dissolved inorganic carbon (DIC), total alkalinity (TA), and $\delta^{13}C_{\rm DIC}$.

DO concentrations were determined within 24 h using automated Winkler titration (precision: 0.1% or \pm 0.23

23782242, 0, Downloaded from https://aslopubs.

onlinelibrary.wiley.com/doi/10.1002/lol2.70055 by Xiamen University, Wiley Online Library on [13/10/2025]. See the Terms

use; OA articles are governed by the applicable Creative Commons License

μmol kg⁻¹) (Dai et al. 2006). Dissolved inorganic carbon concentrations were analyzed by acidifying 0.6 mL seawater samples with phosphoric acid; liberating CO₂ was quantified via a LI-COR 7000 non-dispersive infrared (NDIR) spectrometer (AS-C6L, accuracy \pm 2.0 μmol kg⁻¹) (Cai et al. 2004). Total alkalinity was measured using potentiometric Gran titration (AS-ALK3, accuracy \pm 2.0 μmol kg⁻¹) (Cai et al. 2004). Both DIC and TA measurements were calibrated against certified reference materials (CRMs) from the Scripps Institution of Oceanography. For $\delta^{13}C_{\rm DIC}$ analysis, CO₂ was extracted cryogenically from 3 mL acidified seawater, purified via vacuum distillation, and analyzed by cavity ring-down spectroscopy (Picarro G2131-i; accuracy < 0.1‰) (Chen et al. 2022).

pH was calculated from DIC and TA using the CO2SYS program (Lewis and Wallace 1998), employing carbonic acid dissociation constants (K₁ and K₂) from Lueker et al. (2000), K_{HSO4} dissociation constants from Dickson (1990), and total borate-salinity relationship from Lee et al. (2010). All pH values are reported on the total hydrogen scale (pH_T). While organic alkalinity can contribute to measured TA in aquaculture waters (Xiong et al. 2023) and should be considered, our assessment indicates that this contribution is negligible in the Sansha Bay system (*see* Supporting Information Text S2).

Multi-endmember mixing model

To disentangle physical mixing from biogeochemical processes affecting DIC, TA, DO, and $\delta^{13}C_{DIC}$, we employed a two-endmember mixing model following e.g., Yang et al. (2022) (Cao et al. 2011; Yang et al. 2022):

$$f_1 + f_2 = 1$$
 (1)

$$S_1 \times f_1 + S_2 \times f_2 = S \tag{2}$$

where S denotes salinity, subscripts 1 and 2 denote distinct water mass end-members, with f_1 and f_2 calculated accordingly. Conservative concentrations (DIC^{cons}, DO^{cons}, TA^{cons}) and δ^{13} C_{DIC} were calculated as:

$$DIC^{cons} = DIC_1 \times f_1 + DIC_2 \times f_2 \tag{3}$$

$$DO^{cons} = DO_1 \times f_1 + DO_2 \times f_2 \tag{4}$$

$$TA^{cons} = TA_1 \times f_1 + TA_2 \times f_2 \tag{5}$$

$$\delta^{13}C_{DIC}^{cons} = \left(\delta^{13}C_1 \times DIC_1 \times f_1 + \delta^{13}C_2 \times DIC_2 \times f_2\right) / DIC^{cons}$$
 (6)

Non-conservative deviations ($\Delta DIC = DIC^{obs} - DIC^{cons}$) reflect net biogeochemical alterations (Su et al. 2017; Zhao et al. 2020). The selection of end-members and their corresponding values are detailed in Supporting Information Fig. S2 and Supporting Information Table S4.

Semi-analytical diagnostic method based on DIC and $\delta^{13}C_{\rm DIC}$

Observed vs. modeled discrepancies were attributed to airsea CO_2 exchange (ΔDIC_{as}), biological processes (ΔDIC_{bio}), and calcium carbonate cycling (ΔDIC_{CaCO_3}) (Ouyang et al. 2024; Zhao et al. 2020):

$$\Delta DIC = DIC^{obs} - DIC^{cons} = \Delta DIC_{as} + \Delta DIC_{bio} + \Delta DIC_{CaCO_3}$$
 (7)

$$\delta^{13}C_{obs} \times DIC_{obs} - \delta^{13}C_{cons} \times DIC_{cons} = \Delta DIC_{as} \times \delta^{13}C_{as} + \Delta DIC_{bio} \times \delta^{13}C_{bio} + \Delta DIC_{CaCO_3} \times \delta^{13}C_{CaCO_3}$$
(8)

A systematic analysis of each term in Eqs. 7 and 8 is presented below:

$$\Delta \text{DIC}_{\text{as}} = F_{\text{CO}_2} \times \frac{t}{h} / \rho \tag{9}$$

where F_{CO_2} is air–sea CO₂ flux (mmol m⁻² d⁻¹), t the time interval (days), h the mixed-layer depth (m), and ρ seawater density (kg m⁻³). The isotopic composition of CO₂ (δ^{13} C_{as}) associated with gas exchange was derived as:

$$\delta^{13}C_{CO_2} = \delta^{13}C_{DIC} + 23.644 - \frac{9701.5}{T}$$
 (10)

$$\delta^{13}C_{as} = \delta^{13}C_{atm-CO_2} + \varepsilon \tag{11}$$

where T is temperature (K), $\delta^{13}C_{atm-CO_2} = -8.5\%$ (Keeling et al. 2017), and $\varepsilon = \delta^{13}C_{CO2} - \delta^{13}C_{DIC}$ represents equilibrium fractionation.

We assumed $(\delta^{13}C_{CaCO_3}=0\%)$ for marine limestone (Alling et al. 2012). Since air–sea exchange and biological processes negligibly affect TA, the calculation of ΔDIC_{CaCO_3} is performed using the formula $\Delta DIC_{CaCO_3}=0.5\times\Delta TA$ (Xue et al. 2020). Consequently:

$$\Delta DIC_{bio} = \Delta DIC - \Delta DIC_{as} - \Delta DIC_{CaCO_3}$$
 (12)

The DIC isotopic mass balance (Su et al. 2017) is expressed as

$$\delta^{13}C_{\text{obs}} \times \text{DIC}_{\text{obs}} = \delta^{13}C_{\text{cons}} \times \text{DIC}_{\text{cons}} + \delta^{13}C_{\text{bio}} \times \text{DIC}_{\text{bio}}$$
 (13)

The degradation of OC typically generates DIC with minor isotopic fractionation relative to the original OC substrate (Breteler et al. 2002; Su et al. 2017). Consequently, the isotopic composition of biologically produced DIC ($\delta^{13}C_{\text{bio}}$) is expected to closely reflect that of the source organic carbon ($\delta^{13}C_{\text{OC}}$), which consumed oxygen during its breakdown (Ouyang et al. 2024). The value of $\delta^{13}C_{\text{OC}}$ was estimated using mass balance equations based on both DIC concentration and its stable carbon isotope composition.

Liu et al.

$$\begin{split} \delta^{13}C_{oc} &= \left(\delta^{13}C_{obs} \times DIC_{obs} - \delta^{13}C_{mixing} \times DIC_{mixing} - \Delta DIC_{as} \right. \\ &\times \delta^{13}C_{as} - \Delta DIC_{CaCO_3} \times \delta^{13}C_{CaCO_3}) / \left(DIC^{obs} - DIC^{cons} - \Delta DIC_{as} \right. \\ &\left. - \Delta DIC_{CaCO_3}\right) \end{split}$$

which can be rearranged into

$$\Delta(\delta^{13}C_{DIC} \times DIC) = \delta^{13}C_{OC} \times \Delta DIC_{bio}$$
 (15)

where the left term represents the cumulative isotopic deviation, and the slope of $\Delta(\delta^{13}C_{DIC}\times DIC)$ vs. ΔDIC_{bio} quantifies the $\delta^{13}C$ signature of metabolized organic carbon (Su et al. 2020).

The contribution of organic matter to oxygen-consuming organic matter was estimated using a carbon isotopic mass balance approach, as described by the following equation (Zhao et al. 2020; Hu et al. 2006):

$$f(\%) = (\delta^{13}C_{OC} - \delta^{13}C_1)/(\delta^{13}C_2 - \delta^{13}C_1) \times 100$$
 (16)

where $\delta^{13}C_1$ and $\delta^{13}C_2$ are the representative values of fish feed and macroalgae detritus particulate organic carbon, respectively, at approximately -23.4% (Han et al. 2024) and -16.9% (Han et al. 2024).

Results

Spatial–temporal distributions of oxygen and pH in Sansha Bay and their seasonal evolutions

This study investigates the regulation of the carbonate system across different aquaculture regimes by comparing the main channel of Sansha Bay (non-culture area) with the Dongwuyang embayment (seasonal aquaculture area) (Fig. 2c). In Dongwuyang, aquaculture practices exhibit pronounced seasonal transitions. During autumn, intensive fish farming at the embayment's entrance coincides with the cultivation of *G. lemaneiformis* in the northeast. This is followed by a winter phase dominated by *S. japonica* cultivation—with residual *G. lemaneiformis* beds persisting into the pre-planting phase—and ultimately transitions into a spring period marked by extensive *S. japonica* harvesting.

Our multi-seasonal investigations revealed a pronounced spatial variability in carbonate system parameters that is closely linked to the intensity of macroalgae cultivation and fish farming. During peak aquaculture periods, surface waters generally acted as net $\rm CO_2$ sources, exhibiting elevated $p\rm CO_2$ levels ranging from 412 to 1172 μ atm (Fig. 2a–f), contrary to the anticipated carbon sink behavior. In particular, the northeastern Dongwuyang region, characterized by prolonged water half-exchange time of 15–40 d (Lin et al. 2017), consistently exhibited higher $p\rm CO_2$ levels (672 \pm 167 μ atm) compared to the more rapidly flushed main channel (half-exchange time of 0.5 d; Lin et al. 2017) which maintained $p\rm CO_2$ levels

of $534 \pm 32~\mu$ atm. Our observations of the seasonal evolution of $p\text{CO}_2$ level and CO_2 source-sink status are consistent with carbon fluxes obtained from eddy covariance timeseries measurements in the same region (Deng et al. 2025). Although our ship-based observations were limited in duration and did not capture the expected strong carbon sink during the rapid growth phase of *S. japonica*, the continuous eddy covariance measurements indicate that, aside from a strong carbon sink observed in December, the Sansha Bay aquaculture areas function as carbon sources throughout the remainder of the year, even during periods of ongoing *G. lemaneiformis* cultivation.

Seasonal variations further highlighted the tightly coupled dynamics between DO and carbonate system parameters. In autumn, significant oxygen depletion was observed around aquaculture sites, with DO levels dropping to as low as 74.8% of saturation—approximately 10% lower than in the surrounding reference waters (Fig. 2g), δ¹³C_{DIC} values ranging from -1.83 % to -1.30 %, indicating a depletion of 0.3–0.8 % compared to the Main-channel (Fig. 2j), and pH values between 7.5 and 7.7—roughly 0.2–0.3 units lower than those in adjacent non-culture waters (Fig. 2m). In winter, the photosynthetic activity of macroalgae temporarily alleviated acidification, elevating surface DO to 112.9%, reducing DIC concentration to 1931 μ mol kg⁻¹ (Supporting Information Fig. S3c), and enriching $\delta^{13}C_{DIC}$ values (-0.75% to 0.27%; Fig. 2h,k,n). Conversely, during spring, conditions intensified oxygen depletion, with minimum DO levels reaching only 44% of saturation, DIC concentrations increasing to 2318 μ mol kg⁻¹ (Supporting Information Fig. S3k), and δ^{13} C-DIC values becoming notably depleted (-3.21% to -0.92%; Fig. 2i,l,o). In addition, the relatively high total alkalinity observed in the Dongwuyang area during spring indicates an input of submarine groundwater discharge (SGD), which elevated the baseline TA of the system. In contrast, the main channel, benefiting from rapid water renewal, consistently maintained relatively stable conditions (DO > 85% and DIC < 2095 μ mol kg⁻¹), underscoring the significant influences of aquaculture and hydrodynamic forces on local biogeochemical signals.

Low oxygen and pH throughout the water column in aquaculture areas

Vertical profiles revealed marked differences between aquaculture zones and adjacent non-culture regions. In aquaculture-affected areas, the water column consistently exhibited low oxygen levels and reduced pH, whereas the main channel maintained oxygen-rich conditions (Fig. 3).

In autumn, although the water columns were generally well-mixed (Supporting Information Fig. S4), localized zones of oxygen depletion were persistent near fish farms. This contrasted sharply with macroalgae-dense regions, where active photosynthesis elevated surface dissolved oxygen and pH levels (Fig. 3a–d). During winter, surface photosynthetic activity temporarily boosted oxygen concentrations to 112.9% of

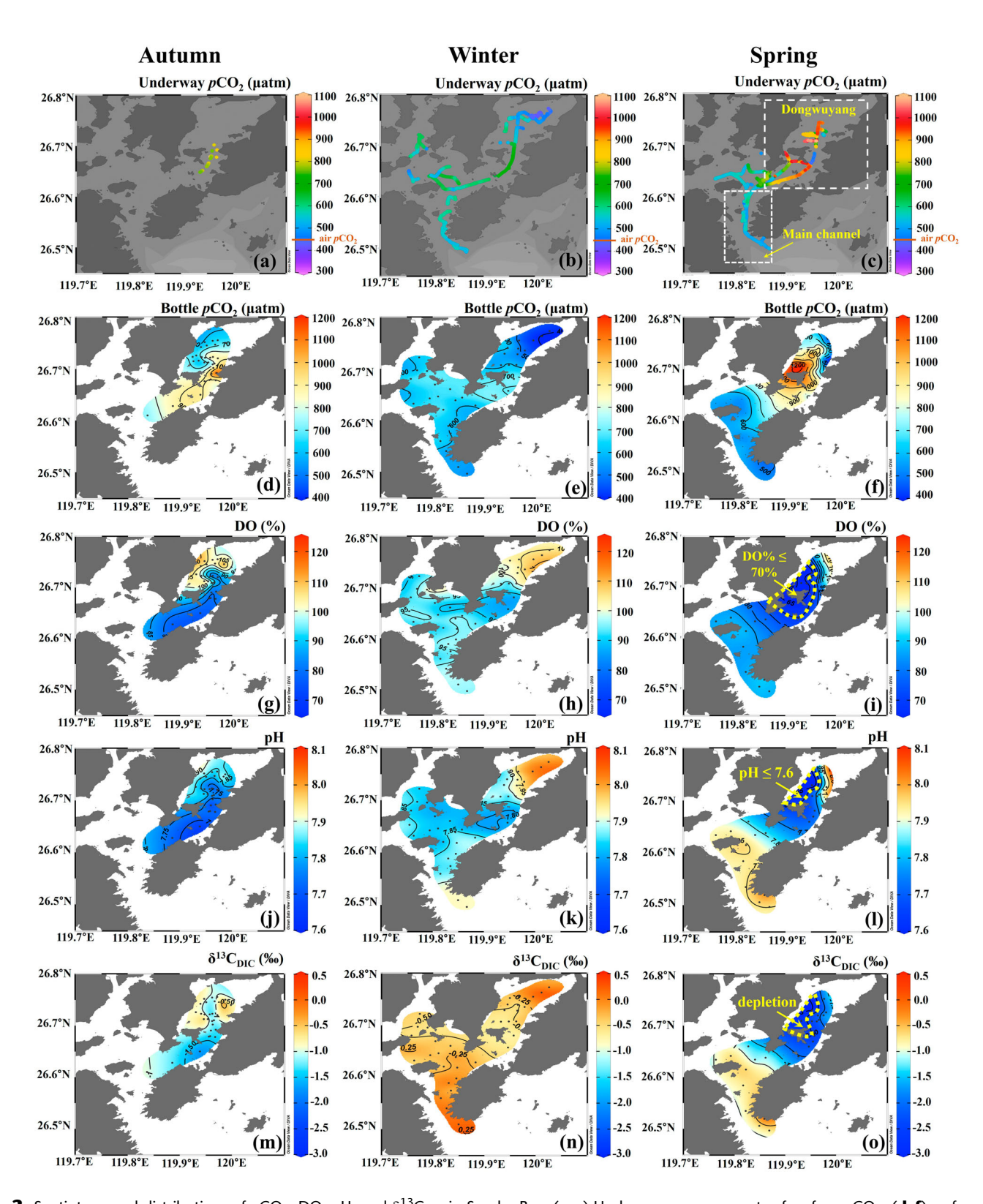


Fig. 2. Spatiotemporal distributions of pCO_2 , DO, pH, and $\delta^{13}C_{DIC}$ in Sansha Bay. (**a–c**) Underway measurements of surface pCO_2 ; (**d–f**) surface pCO_2 derived from discrete bottle samples calculated using CO2SYS; (**g–o**) DO, pH, and $\delta^{13}C_{DIC}$ at the bottom waters. Horizontal distributions of pCO_2 , DO, pH, and $\delta^{13}C_{DIC}$ at the bottom waters. Rows indicate different parameters, and columns indicate different seasons. The white dotted line in (c) divides Sansha Bay into two distinct zones: non-aquaculture area (main channel) and aquaculture-impacted area (Dongwuyang, seaweed farming and fish-macroalgae polyculture system).

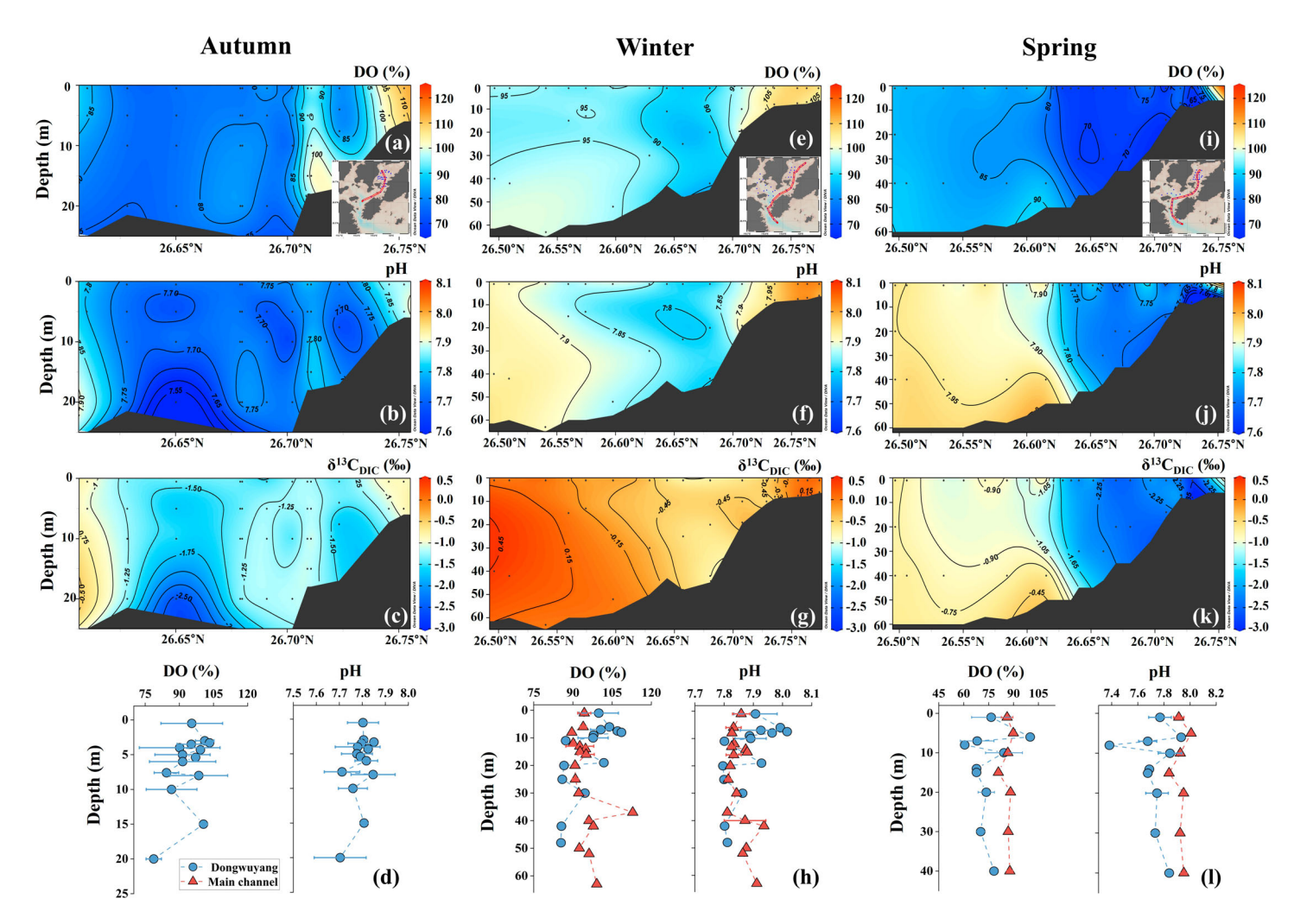


Fig. 3. Seasonal vertical profiles along the main channel–Dongwuyang transect. (**a–c**) autumn, (**e–g**) winter, and (**i–k**) spring profiles of DO, pH, and $\delta^{13}C_{DIC}$. Depth-integrated averages for each season are quantified in (d), (h), and (l).

saturation and increased pH values, while both parameters remained low in the subsurface (≥20 m depth), comparable to or lower than those observed in the main channel (Fig. 3h).

In spring, the entire water column of northeastern Dongwuyang was dominated by severe hypoxia (DO ranging from 44% to 70% of saturation) and acidification (pH between 7.4 and 7.6), along with pronounced depletion of $\delta^{13}C_{\rm DIC}$ values (–3.2% to –2.5%; Fig. 3i–k). Winddriven vertical mixing played a key role by transporting degradation byproducts from organic-rich sediments upward, as indicated by the observed hypoxic gradients and carbon isotope fractionation.

Discussion and conclusion

Partitioning source of decomposed organic carbon inducing hypoxia and acidification

Deviations in DIC, pH, and $\delta^{13}C_{DIC}$ from conservative mixing models exhibited clear seasonal patterns. In winter,

we observed net DIC consumption accompanied by increased pH (Supporting Information Fig. S5). In contrast, both autumn and spring were characterized by elevated DIC, lower pH, and depleted $\delta^{13}C_{DIC}$ values (Supporting Information Fig. S5), indicating that OC remineralization following algae growth is the primary driver of these changes (Hullar et al. 1996; Breteler et al. 2002).

In this seaweed farming system, OC is derived from both marine and terrestrial sources. Using the DIC isotopic mass balance (Eq. 15), we determined the δ^{13} C signatures of decomposed OC driving DIC production and oxygen consumption, with values of -22.6% in autumn and -19.1% in spring (Supporting Information Fig. 4). These values differ markedly from terrestrial OC signatures (-28.6%; Zhao et al. 2020) and closely resemble those of marine sources (-20.6%; Zhao et al. 2020), indicating that marine-derived OC decomposition dominates. Although limited sampling near riverine inputs constrains accurate estimation of marine vs. terrestrial contributions, evidence suggests that the Jiaoxi

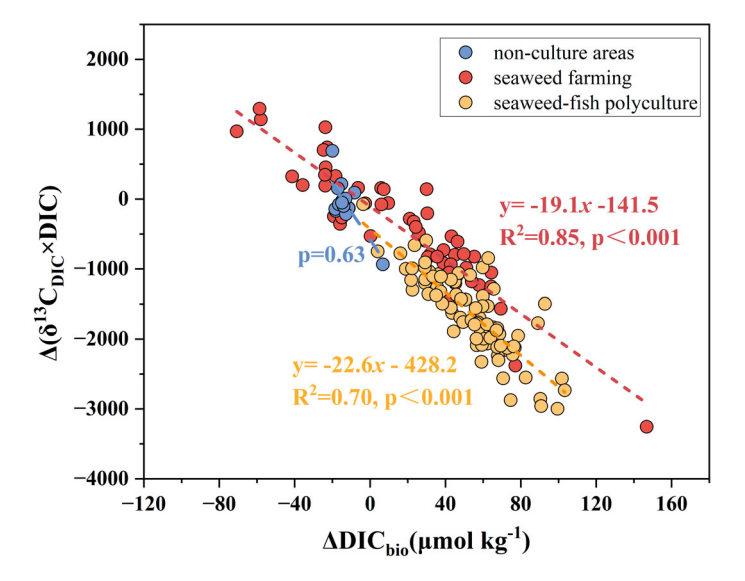


Fig. 4. Relationships between ΔDIC_{bio} and $\Delta (\delta^{13}C_{DIC} \times DIC)$. ΔDIC_{bio} denotes the biologically-induced change in DIC, whereas $\Delta (\delta^{13}C_{DIC} \times DIC)$ reflects deviations of $\delta^{13}C_{DIC} \times DIC$ from conservative mixing. Symbols distinguish among the following regions/seasons: nonculture main channel areas in spring (blue), seaweed culture in Dongwuyang in spring (red), and seaweed-fish polyculture in Dongwuyang in autumn (yellow). The dashed lines represent linear regressions for different sets, with slopes indicating the $\delta^{13}C$ signatures of degraded organic carbon. Note that the regression fit for non-culture areas is statistically insignificant.

River is the primary terrestrial source to Sansha Bay; however, its distance from the Dongwuyang study area minimizes terrestrial influence due to geomorphic isolation (Fig. 1b; Han et al. 2021; Wang et al. 2015; Zhang et al. 2024).

Furthermore, we differentiated between fish and algal sources within the marine OC pool. In autumn, $\delta^{13}C_{OC}$ values (–22.6%; Fig. 4) align with signals from fish feed decomposition (characterized by value of –23.4‰ as reported by Han et al. 2024), accounting for approximately 88% of DIC accumulation (Eq. 16). In spring, values (–19.1‰; Fig. 4) shift toward macroalgal detritus signatures (–16.9‰; Han et al. 2024), with algal-derived carbon contributing about 66% to DIC enrichment (Eq. 16). This seasonal transition, from fish-driven carbon dynamics in autumn to macroalgal detritus dominance in spring (Fig. 4), highlights a previously overlooked aspect of polyculture operations.

Complexity and implications of polyculture

Our results challenge the conventional view of integrated aquaculture as a straightforward carbon mitigation strategy. Although macroalgal photosynthesis temporarily reduces CO_2 levels during its peak growth in winter (Deng et al. 2025), our comprehensive analyses consistently reveal a net CO_2 release in other seasons, primarily driven by the decomposition of macroalgal detritus and fish feed (Fig. 4).

Hydrodynamic conditions critically reinforce these impacts. In contrast to wild algal forests or open systems that maintain a wider and unrestricted connection to the open ocean—allowing macroalgal detritus to be transported over large distances within days to weeks (Boyd et al. 2022)—the restricted water exchange in Sansha Bay (Fig. 1b) results in nearly complete local decomposition of organic debris, typically over timescales of 6–70 d, with a peak around 15 d (Liu et al. 2016; Luo et al. 2023; Smith and Foreman 1984) (Supporting Information Fig. S6). This temporal alignment between water retention and organic decay intensifies

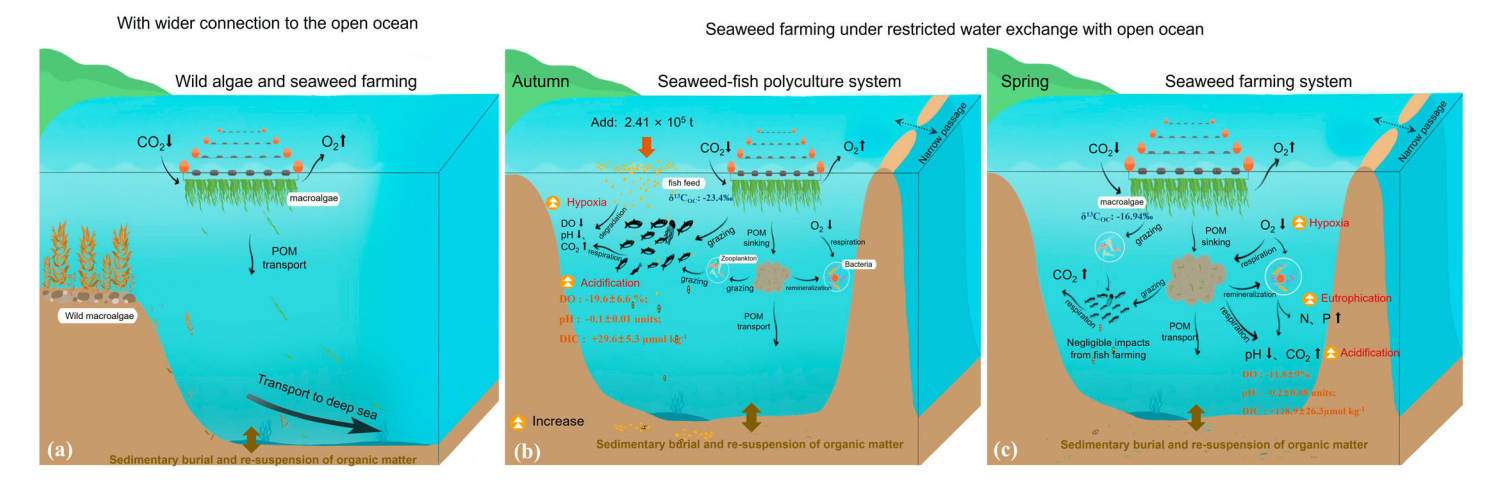


Fig. 5. Schematic illustrating the different biogeochemical drivers in the highly sheltered Sansha Bay seaweed farming area with a lagoon-like geographic configuration, as well as a comparison to the relatively open systems of wild algae and seaweed cultivation. (a) Wild algae and seaweed farming system with a wider connection to the open ocean. (b) Autumn scenario dominated by fish feed inputs, leading to localized oxygen depletion and acidification, establishing surface waters as a net CO₂ source. (c) Spring scenario primarily controlled by macroalgal detritus decomposition, with surface waters acting as a net CO₂ source as well. The net changes in DO, pH, and DIC during seaweed farming and fish polyculture presented in (b) and (c) are derived from aquaculture zones, with the main channel serving as a baseline.

negative impacts, including hypoxia, acidification, and eutrophication. Both the expansion of seaweed farming and the prolonged water retention time are significant contributing factors to hypoxia and acidification in the study area. Although current DO levels (minimum: 44.0%) have not yet reached severe hypoxia thresholds (< 26.5% at 25°C), they already compromise ecosystem function and may serve as precursors to more severe conditions, particularly during summer stratification. In contrast, another typical partially sheltered aquaculture region, Sanggou Bay in Northeast China—where similar large-scale macroalgal aquaculture is practiced without fish polyculture but maintains stronger water exchange through its semi-open connection to the adjacent ocean—consistently functions as a strong carbon sink throughout the year (Han et al. 2025).

Our conceptual model (Fig. 5) integrates seasonal interactions across different aquaculture scenarios, clarifying the combined impacts of seaweed and fish farming on key biogeochemical parameters such as DIC, DO, and pH. The seasonal progression, shifting from fish feed decomposition in autumn to macroalgal detritus decomposition in spring, explains the transition from transient photosynthetic CO₂ uptake to sustained heterotrophic CO₂ release. These findings highlight the need for aquaculture management strategies that address both biological production phases and hydrodynamic constraints. Measures such as reducing cultivation densities and improving water exchange are essential to prevent irreversible hypoxia and acidification in semi-enclosed bays. Without proactive intervention, intensive aquaculture sites such as Sansha Bay may develop chronic hypoxic conditions similar to those observed in severely impacted estuarine environments such as the Yangtze and Pearl River estuaries (Cui et al. 2019; Wang et al. 2017). Future aquaculture management should consider both carbon sequestration capacity and ecosystem health to ensure sustainable and resilient environments.

Author Contributions

Yingxu Wu and Di Qi designed the study. Yanmei Liu, Wei Yang, and Yingxu Wu processed and analyzed data. Yanmei Liu wrote the original manuscript. Yanmei Liu, Wei Yang, and Yingxu Wu made the figures. All the authors contributed to the writing and revision of the manuscript. Yanmei Liu and Wei Yang contributed equally to this study.

Acknowledgments

This work was supported by the Ocean Negative Carbon Emissions (ONCE) Program. This work was also funded by the National Key Research and Development Program of China (2023YFC3108102), the Natural Science Foundation of Fujian Province (2025J09045, 2022J01818, 2023J01797,

2024J01114), the 2024 International Cooperation Seed Funding Project for China's Ocean Decade Actions (Grant GHZZ3702840002024020000028), the Science Foundation of Xiamen, Fujian Province (Grant 3502Z20227051), and the Science Foundation of Fujian Educational Bureau (Grant JAT220178).

Conflicts of Interest

None declared.

Data Availability Statement

Data and metadata are available in the Mendeley Data repository, at https://data.mendeley.com/datasets/ykd3kv453d/1.

References

Alling, V., D. Porcelli, C. M. Mörth, et al. 2012. "Degradation of Terrestrial Organic Carbon, Primary Production and Out-Gassing of CO_2 in the Laptev and East Siberian Seas as Inferred From $\delta^{13}C$ Values of DIC." *Geochimica et Cosmochimica Acta* 95: 143–159. https://doi.org/10.1016/j. gca.2012.07.028.

Bach, L. T., V. Tamsitt, J. Gower, C. L. Hurd, J. A. Raven, and P. W. Boyd. 2021. "Testing the Climate Intervention Potential of Ocean Afforestation Using the Great Atlantic Sargassum Belt." *Nature Communications* 12, no. 1: 2556. https://doi.org/10.1038/s41467-021-22837-2.

Boyd, P. W., L. T. Bach, C. L. Hurd, E. Paine, J. A. Raven, and V. Tamsitt. 2022. "Potential Negative Effects of Ocean Afforestation on Offshore Ecosystems." *Nature Ecology & Evolution* 6, no. 6: 675–683. https://doi.org/10.1038/s41559-022-01722-1.

Breteler, W. C. M. K., K. Grice, S. Schouten, H. T. Kloosterhuis, and J. S. Sinninghe Damsté. 2002. "Stable Carbon Isotope Fractionation in the Marine Copepod Temora Longicornis: Unexpectedly Low δ^{13} C Value of Faecal Pellets." *Marine Ecology Progress Series* 240: 195–204. https://doi.org/10.3354/meps240195.

Cai, W.-J., M. Dai, Y. Wang, et al. 2004. "The Biogeochemistry of Inorganic Carbon and Nutrients in the Pearl River Estuary and the Adjacent Northern South China Sea." *Continental Shelf Research* 24, no. 12: 1301–1319. https://doi.org/10.1016/j.csr.2004.04.005.

Cao, Z., M. Dai, N. Zheng, et al. 2011. "Dynamics of the Carbonate System in a Large Continental Shelf System Under the Influence of Both a River Plume and Coastal Upwelling." *Journal of Geophysical Research* 116, no. G2: G02010. https://doi.org/10.1029/2010JG001596.

Chen, Z.-y., W.-d. Zhai, S. Yang, Y. Zhang, and P.-f. Liu. 2022. "Exploring Origin of Oxygen-Consuming Organic Matter in a Newly Developed Quasi-Hypoxic Coastal Ocean, the Bohai Sea (China): A Stable Carbon Isotope Perspective."

- Science of the Total Environment 837: 155847. https://doi.org/10.1016/j.scitotenv.2022.155847.
- Cui, Y., J. Wu, J. Ren, and J. Xu. 2019. "Physical Dynamics Structures and Oxygen Budget of Summer Hypoxia in the Pearl River Estuary." *Limnology and Oceanography* 64, no. 1: 131–148. https://doi.org/10.1002/lno.11025.
- Dai, M., X. Guo, W. Zhai, et al. 2006. "Oxygen Depletion in the Upper Reach of the Pearl River Estuary During a Winter Drought." *Marine Chemistry* 102, no. 1: 159–169. https://doi.org/10.1016/j.marchem.2005.09.020.
- Deng, Y., X. Guo, X. Zhao, et al. 2025. "Coastal Macroalgae Aquaculture Reduces Carbon Dioxide Emission in a Subtropical Enclosed Bay: Insights From Eddy Covariance Measurements." *Agriculture, Ecosystems & Environment* 385: 109576. https://doi.org/10.1016/j.agee.2025.109576.
- Dickson, A. G. 1990. "Thermodynamics of the Dissociation of Boric Acid in Synthetic Seawater From 273.15 to 318.15 K." *Deep Sea Research Part A. Oceanographic Research Papers* 37, no. 5: 755–766. https://doi.org/10.1016/0198-0149(90) 90004-F.
- Doney, S. C., W. H. Wolfe, D. C. McKee, and J. G. Fuhrman. 2025. "The Science, Engineering, and Validation of Marine Carbon Dioxide Removal and Storage." *Annual Review of Marine Science* 17, no. 1: 55–81. https://doi.org/10.1146/annurev-marine-040523-014702.
- Du, J., J. Shen, K. Park, Y. P. Wang, and X. Yu. 2018. "Worsened Physical Condition Due to Climate Change Contributes to the Increasing Hypoxia in Chesapeake Bay." *Science of the Total Environment* 630: 707–717. https://doi.org/10.1016/j.scitotenv.2018.02.265.
- Duarte, C. M., A. Bruhn, and D. Krause-Jensen. 2021. "A Seaweed Aquaculture Imperative to Meet Global Sustainability Targets." *Nature Sustainability* 5, no. 3: 185–193. https://doi.org/10.1038/s41893-021-00773-9.
- Duarte, C. M., A. Delgado-Huertas, E. Marti, et al. 2025. "Carbon Burial in Sediments Below Seaweed Farms Matches That of Blue Carbon Habitats." *Nature Climate Change* 15, no. 2: 180–187. https://doi.org/10.1038/s41558 -024-02238-1.
- Filbee-Dexter, K., A. Pessarrodona, M. F. Pedersen, et al. 2024. "Carbon Export from Seaweed Forests to Deep Ocean Sinks." *Nature Geoscience* 17, no. 6: 552–559. https://doi.org/10.1038/s41561-024-01449-7.
- Friedlingstein, P., M. O'Sullivan, M. W. Jones, et al. 2025. "Global Carbon Budget 2024." *Earth System Science Data* 17, no. 3: 965–1039. https://doi.org/10.5194/essd-17-965-2025.
- Gallagher, J. B., V. Shelamoff, C. Layton. 2022. "Seaweed Ecosystems may not Mitigate CO2 Emissions." *ICES Journal of Marine Science* 79, no. 3: 585–592.
- Gattuso, J. P., A. Magnan, R. Billé, et al. 2015. "Contrasting Futures for Ocean and Society From Different Anthropogenic CO₂ Emissions Scenarios." *Science* 349,

- no. 6243: aac4722. https://doi.org/10.1126/science.aac4722.
- Han, A., J. Y. T. Yang, M. l. Chen, et al. 2024. "Hydrological Connectivity Controls on the Dynamics of Particulate Organic Matter in a Semi-Enclosed Mariculture Bay." *Aquaculture* 578: 740109. https://doi.org/10.1016/j.aquaculture. 2023.740109.
- Han, A., S. J. Kao, W. f. Lin, et al. 2021. "Nutrient Budget and Biogeochemical Dynamics in Sansha Bay, China: A Coastal Bay Affected by Intensive Mariculture." *Journal of Geophysical Research: Biogeosciences* 126, no. 9: e2020JG006220. https://doi.org/10.1029/2020JG006220.
- Han, T., R. Shi, Z. Qi, Q. Liu, and H. Huang. 2025. "Role of Intensive Mariculture on CO₂ Absorption and Carbon Burial, and the Carbon Sink Potential of Sanggou Bay, China." *Aquaculture* 597: 741936. https://doi.org/10.1016/j.aquaculture.2024.741936.
- Hu, J., P. a. Peng, G. Jia, B. Mai, and G. Zhang. 2006. "Distribution and Sources of Organic Carbon, Nitrogen and Their Isotopes in Sediments of the Subtropical Pearl River Estuary and Adjacent Shelf, Southern China." *Marine Chemistry* 98, no. 2: 274–285. https://doi.org/10.1016/j.marchem.2005.03.008.
- Hu, Z., J. W. Lee, K. Chandran, S. Kim, and S. K. Khanal. 2012. "Nitrous Oxide (N₂O) Emission From Aquaculture: A Review." *Environmental Science & Technology* 46, no. 12: 6470–6480. https://doi.org/10.1021/es300110x.
- Hullar, M., B. Fry, B. J. Peterson, and R. T. Wright. 1996. "Microbial Utilization of Estuarine Dissolved Organic Carbon: A Stable Isotope Tracer Approach Tested by Mass Balance." *Applied and Environmental Microbiology* 62, no. 7: 2489–2493. https://doi.org/10.1128/aem.62.7.2489-2493. 1996.
- Ji, W., H. Yokoyama, J. Fu, and J. Zhou. 2021. "Effects of Intensive Fish Farming on Sediments of a Temperate Bay Characterised by Polyculture and Strong Currents." *Aquaculture Reports* 19: 100579. https://doi.org/10.1016/j.aqrep. 2020.100579.
- Jiang, Z., J. Liu, J. Chen, et al. 2014. "Responses of Summer Phytoplankton Community to Drastic Environmental Changes in the Changjiang (Yangtze River) Estuary During the Past 50 Years." *Water Research* 54: 1–11. https://doi.org/10.1016/j.watres.2014.01.032.
- Keeling, R. F., H. D. Graven, L. R. Welp, et al. 2017. "Atmospheric Evidence for a Global Secular Increase in Carbon Isotopic Discrimination of Land Photosynthesis." *Proceedings of the National Academy of Sciences of the United States of America* 114, no. 39: 10361–10366. https://doi.org/10.1073/pnas.1619240114.
- Krause-Jensen, D., and C. M. Duarte. 2016. "Substantial Role of Macroalgae in Marine Carbon Sequestration." *Nature Geoscience* 9, no. 10: 737–742. https://doi.org/10.1038/nge o2790.

- Krause-Jensen, D., P. Lavery, O. Serrano, N. Marba, P. Masque, and C. M. Duarte. 2018. "Sequestration of Macroalgal Carbon: The Elephant in the Blue Carbon Room." *Biology Letters* 14, no. 6: 20180236. https://doi.org/10.1098/rsbl.2018. 0236.
- Lee, K., T.-W. Kim, R. H. Byrne, F. J. Millero, R. A. Feely, and Y.-M. Liu. 2010. "The Universal Ratio of Boron to Chlorinity for the North Pacific and North Atlantic Oceans." *Geochimica et Cosmochimica Acta* 74, no. 6: 1801–1811. https://doi.org/10.1016/j.gca.2009.12.027.
- Lewis, E. R., and D. W. R. Wallace. 1998. "Program Developed for CO₂ System Calculations." In *ORNL/CDIAC-105*. Environmental System Science Data Infrastructure for a Virtual Ecosystem. https://doi.org/10.1364/ao.37.005985.
- Lin, H., Z. Chen, J. Hu, et al. 2017. "Numerical Simulation of the Hydrodynamics and Water Exchange in Sansha Bay." *Ocean Engineering* 139: 85–94. https://doi.org/10.1016/j.oceaneng.2017.04.031.
- Lin, H., Z. Chen, J. Hu, et al. 2019. "Impact of Cage Aquaculture on Water Exchange in Sansha Bay." *Continental Shelf Research* 188: 103963. https://doi.org/10.1016/j.csr.2019. 103963.
- Liu, X., Z. Wang, and X. Zhang. 2016. "A Review of the Green Tides in the Yellow Sea, China." *Marine Environmental Research* 119: 189–196. https://doi.org/10.1016/j.marenv res.2016.06.004.
- Lueker, T. J., A. G. Dickson, and C. D. Keeling. 2000. "Ocean *p*CO₂ Calculated from Dissolved Inorganic Carbon, Alkalinity, and Equations for K1 and K2: Validation Based on Laboratory Measurements of CO₂ in Gas and Seawater at Equilibrium." *Marine Chemistry* 70, no. 1: 105–119. https://doi.org/10.1016/S0304-4203(00) 00022-0.
- Luo, H., Y. Yang, and S. Xie. 2023. "The Ecological Effect of Large-Scale Coastal Natural and Cultivated Seaweed Litter Decay Processes: An Overview and Perspective." *Journal of Environmental Management* 341: 118091. https://doi.org/10.1016/j.jenvman.2023.118091.
- McNeary, W. W., and L. E. Erickson. 2013. "Sustainable Management of Algae in Eutrophic Ecosystems." *Journal of Environmental Protection* 04, no. 11: 9–19. https://doi.org/10.4236/jep.2013.411A002.
- Officer, C. B., R. B. Biggs, J. L. Taft, L. E. Cronin, M. A. Tyler, and W. R. Boynton. 1984. "Chesapeake Bay Anoxia: Origin, Development, and Significance." *Science* 223, no. 4631: 22–27. https://doi.org/10.1126/science.223.4631.22.
- Ouyang, Z., A. Fujiwara, S. Nishino, et al. 2024. "Source Partitioning of Dissolved Inorganic Carbon Addition to Pacific Winter Water in the Western Arctic Ocean." *Limnology and Oceanography* 69, no. 11: 2532–2546. https://doi.org/10.1002/lno.12684.
- Paine, E. R., M. Schmid, P. W. Boyd, G. Diaz-Pulido, and C. L. Hurd. 2021. "Rate and Fate of Dissolved Organic Carbon Release by Seaweeds: A Missing Link in the Coastal Ocean

- Carbon Cycle." *Journal of Phycology* 57, no. 5: 1375–1391. https://doi.org/10.1111/jpy.13198.
- Saba, G. K., A. B. Burd, J. P. Dunne, et al. 2021. "Toward a Better Understanding of Fish-Based Contribution to Ocean Carbon Flux." *Limnology and Oceanography* 66, no. 5: 1639–1664. https://doi.org/10.1002/lno.11709.
- Smith, B. D., and R. E. Foreman. 1984. "An Assessment of Seaweed Decomposition Within a Southern Strait of Georgia Seaweed Community." *Marine Biology* 84, no. 2: 197–205. https://doi.org/10.1007/BF00393005.
- Su, J., M. Dai, B. He, et al. 2017. "Tracing the Origin of the Oxygen-Consuming Organic Matter in the Hypoxic Zone in a Large Eutrophic Estuary: The Lower Reach of the Pearl River Estuary, China." *Biogeosciences* 14, no. 18: 4085–4099. https://doi.org/10.5194/bg-14-4085-2017.
- Su, J., W.-J. Cai, J. Brodeur, et al. 2020. "Source Partitioning of Oxygen-Consuming Organic Matter in the Hypoxic Zone of the Chesapeake Bay." *Limnology and Oceanography* 65, no. 8: 1801–1817. https://doi.org/10.1002/lno.11419.
- Wang, B., J. Chen, H. Jin, H. Li, D. Huang, and W.-J. Cai. 2017. "Diatom Bloom-Derived Bottom Water Hypoxia off the Changjiang Estuary, With and Without Typhoon Influence." *Limnology and Oceanography* 62, no. 4: 1552–1569. https://doi.org/10.1002/lno.10517.
- Wang, G., Z. Wang, W. Zhai, et al. 2015. "Net Subterranean Estuarine Export Fluxes of Dissolved Inorganic C, N, P, Si, and Total Alkalinity Into the Jiulong River Estuary, China." *Geochimica et Cosmochimica Acta* 149: 103–114. https://doi.org/10.1016/j.gca.2014.11.001.
- Wang, H., M. Dai, J. Liu, et al. 2016. "Eutrophication-Driven Hypoxia in the East China Sea Off the Changjiang Estuary." *Environmental Science & Technology* 50, no. 5: 2255–2263. https://doi.org/10.1021/acs.est.5b06211.
- Wang, H., X. Hu, N. N. Rabalais, and J. Brandes. 2018. "Drivers of Oxygen Consumption in the Northern Gulf of Mexico Hypoxic Waters—A Stable Carbon Isotope Perspective." *Geophysical Research Letters* 45, no. 19: 10528–10538. https://doi.org/10.1029/2018GL078571.
- Wang, Y., W. Yang, Y. Cai, et al. 2023. "Macroalgae Culture-Induced Carbon Sink in a Large Cultivation Area of China." *Environmental Science and Pollution Research* 30, no. 49: 107693–107702. https://doi.org/10.1007/s11356-023-29985-6.
- Wang, Y., X. Guo, G. Wang, et al. 2024. "Assessment of Nutrient Cycling in an Intensive Mariculture System." *Marine Pollution Bulletin* 209: 117085. https://doi.org/10.1016/j.marpolbul.2024.117085.
- Xie, B., H. Cheng, W. Ya, et al. 2021. "Trophic Gauntlet Effects on Fisheries Recovery: A Case Study in Sansha Bay, China." *Ecosystem Health and Sustainability* 7, no. 1: 1965035. https://doi.org/10.1080/20964129.2021.196 5035.
- Xie, B., X. Zhou, L. Huang, et al. 2022. "The Ecological Functions and Risks of Expansive Bivalve-Macroalgae

- Polyculture: A Case Study in Sansha Bay, China." *Aquaculture* 560: 738549. https://doi.org/10.1016/j.aquaculture. 2022.738549.
- Xiong, T. Q., H. M. Li, Y. B. Hu, et al. 2024. "Seaweed Farming Environments Do Not Always Function as CO₂ Sink Under Synergistic Influence of Macroalgae and Microorganisms." *Agriculture, Ecosystems & Environment* 361: 108824. https://doi.org/10.1016/j.agee.2023.108824.
- Xiong, T., H. Li, Y. Yue, et al. 2023. "Legacy Effects of Late Macroalgal Blooms on Dissolved Inorganic Carbon Pool Through Alkalinity Enhancement in Coastal Ocean." *Environmental Science & Technology* 57, no. 5: 2186–2196. https://doi.org/10.1021/acs.est.2c09261.
- Xue, L., X. Yang, Y. Li, et al. 2020. "Processes Controlling Sea Surface pH and Aragonite Saturation State in a Large Northern Temperate Bay: Contrasting Temperature Effects." *Journal of Geophysical Research: Biogeosciences* 125, no. 7: e2020JG005805. https://doi.org/10.1029/2020JG005805.
- Yang, W., X. Guo, Z. Cao, et al. 2022. "Carbonate Dynamics in a Tropical Coastal System in the South China Sea Featuring Upwelling, River Plumes and Submarine Groundwater Discharge." *Science China Earth Sciences* 65, no. 12: 2267–2284. https://doi.org/10.1007/s11430-021-9963-8.
- Zhang, X., Z. Wang, H. Cai, et al. 2022. "Summertime Dissolved Oxygen Concentration and Hypoxia in the Zhejiang

- Coastal Area." *Frontiers in Marine Science* 9: 1051549. https://doi.org/10.3389/fmars.2022.1051549.
- Zhang, Z., F. Wang, L. Lei, N. Zheng, Z. Shen, and J. Mu. 2024. "Spatio-Temporal Dynamics of the Carbonate System During Macroalgae Farming Season in a Semi-Closed Bay in Southeast China." *Frontiers in Marine Science* 11: 1375839. https://doi.org/10.3389/fmars.2024.1375839.
- Zhao, Y., J. Liu, K. Uthaipan, et al. 2020. "Dynamics of Inorganic Carbon and pH in a Large Subtropical Continental Shelf System: Interaction Between Eutrophication, Hypoxia, and Ocean Acidification." *Limnology and Oceanography* 65, no. 6: 1359–1379. https://doi.org/10.1002/lno.11393.
- Zheng, G., and P. M. DiGiacomo. 2020. "Linkages Between Phytoplankton and Bottom Oxygen in the Chesapeake Bay." *Journal of Geophysical Research: Oceans* 125, no. 2: e2019JC015650. https://doi.org/10.1029/2019JC015650.

Supporting Information

Additional Supporting Information may be found in the online version of this article.

Submitted 11 April 2025 Revised 21 July 2025 Accepted 06 August 2025